International Journal of GEOMATE, March., 2018 Vol.14, Issue 43, pp.55-62
Geotec., Const. Mat. & Env., DOI: https://doi.org/10.21660/2018.43.3547
ISSN: 2186-2982 (Print), 2186-2990 (Online), Japan

DEVELOPMENT OF SPECIFIC ELECTROCHEMICAL BIOSENSOR BASED ON CHITOSAN MODIFIED SCREEN PRINTED CARBON ELECTRODE FOR THE MONITORING OF CAPTAN FUNGICIDE

*Porntip Wongkaew[1], Buddhapala Wongkaew[2], Suwita Saepaisan[1], and Panupong Thanutong[2]

[1]Faculty of Agriculture, Khon Kaen University, Khon Kaen 40002, Thailand;
[2]Metropolitan Waterworks Authority, Bangkok 10210, Thailand.

*Corresponding Author, Received: 29 May 2017, Revised: 18 Oct. 2017, Accepted: 1 Dec. 2017

ABSTRACT: Harmful chemicals predominantly used in modern agriculture for pest control have raised a long-term accumulation in the environment and serious problems concerning food safety and health. Excellent detection tools for environmental monitoring are thus urgently needed. The recent biosensor technology is proposed to fulfill this purpose. In this study, an expedient biosensor for captan fungicide determination has been fabricated using its specific reacting enzyme glutathione-s-transferase (GST) covalently immobilized on natural biopolymer chitosan (Chi). The screen-printed carbon electrode (SPCE) has been selected as a basal platform for the biosensor development. Modification of SPCE was made by self-assembled deposition of 1% chitosan in 1% acetic acid solution onto the basal SPCE. Progressive characteristics of the assembled SPCE-Chi-GST have been clearly approved by atomic force microscopy, impedance spectroscopy and cyclic voltammetry (CV). Two sequential oxidation peak currents arose in the electrochemical behavior analysis of captan in the presence of GST substrate electrolyte solution by CV and linear sweep voltammetry (LSV). Dose-response to various captan concentrations was investigated in the range 0 – 20 µg/ml by LSV and a similar good linear relationship between peak current and concentration of captan could be obtained by both oxidation steps with the limit of detection (LOD) at 0.2 µg/ml. Thus the sensitive, rapid, inexpensive and miniature quantitative system for captan monitoring could now be successfully achieved by this proposed biosensor.

Keywords: Electrochemical biosensor · Screen-printed electrode · Captan · Chitosan · Glutathione-s-transferase · Voltammetry

1. INTRODUCTION

The fungicide captan is one of the most frequently applied pesticides belonged to the dicarboximide chemical family containing a chloroalkylthio group. Because of its broad actions, captan has been widely used in a variety of crop production at every growing stage of plant and in various industries including household applications. It is highly toxic to very highly toxic to livestock, poultry, and fish [1]. The evidence of human cardiotoxic effects has also been reported in a rare case of captan ingestion by a skinny person [2]. The acceptable daily intake and acute reference dose of 0.1 and 0.3 mg per kg body weight per day for human have been announced in accordance with the World Health Organization (WHO) to prevent vulnerable effects of threatened captan [3]. Overuse of captan has several drawbacks including pollution in the environment and water ecosystem which in turn a serious risk to animals and human health from either direct exposure or through residues in food and drinking water.

The toxicity of captan is primarily due to an inhibitory effect on enzymes and essential amino compounds production according to several toxicokinetic studies [4]. In captan metabolism, a major functional group, trichloromethylthio ($SCCl_3$) is generally metabolized to the reactive thiophosgene ($S=CCl_2$) along with a relatively stable 1,2,3,6-tetrahydrophthalimide (THPI) in the presence of exposed thiol group. While a cellular detoxification response against this xenobiotic is activated through an enzyme glutathione-s-transferase (GST) that metabolizes a broad range of electrophilic substrates via glutathione (GSH) conjugation. This principal role of GST in xenobiotic-GSH conjugation especially in the reaction with transient thiophosgene to form a product thiazolidine-2-thione-4-carboxylic acid (TTCA) thus has been considered as a basis for captan determination using the electrochemical technique. Even though several reliable methods for the detection are available at presents such as gas chromatography (GC) and high-performance liquid chromatography (HPLC), in coupled with mass spectrometry (MS) but these systems are very sophisticated, highly expensive, laborious and time-consuming. Electrochemical sensor using enzyme reaction is one among advanced effective

tools alternative to such conventional methods. A field-based and in situ environmental monitoring is expected to handle easily on site with several order lower cost by this novel approach.

Our previous studies presented an approved effective and afford able electrochemical implement by a combination of a screen printed carbon electrode (SPCE) and biopolymer chitosan [5]. In this present study, an electrochemical probe based on chitosan modified screen-printed carbon electrode (SPCE-Chi) was employed for a novel fabrication of GST based biosensor. Characterization of the prepared electrodes was carried out using atomic force microscopy (AFM), electrochemical impedance spectroscopy (EIS), and cyclic voltammetry (CV). Statistics calibration was subsequently explored by linear sweep voltammetry (LSV) with varying captan concentration. The present issue also firstly demonstrates the catalytic ability of this SPCE-Chi-GST in the oxidation of captan that liberated significant two sensing mechanisms owning to the simultaneous formation of two different electrophilic complexes from a distinct function of xenobiotic-GSH conjugation.

2. MATERIALS AND METHODS

2.1 Materials and Apparatus

Chitosan (85% degree of deacetylation) with a molecular weight of 0.28 kDa was obtained from Bioline Lab, Co., Thailand. Glutathione-S-transferase from the equine liver, glutathione (GSH) and captan were purchased from Sigma-Aldrich Co. LLC, USA. Other chemicals for reagent preparation were purchased from Ajax Finechem Pty, Ltd., Australia. All solutions and reagents were prepared using high purity deionized water of 18.2 MΩ from Milli-Q RG system (Millipore Corporation, MA, USA.). Screen printed carbon electrode DRP-150 was provided by DropSens, ParqueTecnológico de Asturias, S.L. Llanera (Asturias) Spain. An XE-120 Atomic force microscope (Park Systems Corp., Suwon, Korea) was acquired for electrode surface observation and a PGSTAT 302N ECoChemie Autolab (Metrohm Autolab B.V., Utrecht, The Netherlands) was used for electrochemical analyses.

2.2 Modification of Working Electrode and Fabrication of GST Enzyme-Based Biosensor

Modification of working electrode was performed by self-assembled deposition of chitosan onto an SPCE as previously developed [3]. Fabrication of the enzyme biosensor was executed following an immobilization of GST enzyme (3 U) on SPCE-Chi via the incorporation of glutaraldehyde covalent attachment to ensure the stability of GST as previously described [5].

2.3 Atomic Force Microscopic Observation

Morphological characteristics at nanoscale of original SPCE, SPCE-Chi, and SPCE-Chi-GST working surfaces were allocated by a true noncontact mode AFM with a PPP-NCHR silicon cantilever of < 10 nm tip radius baring a spring constant of 42 N/m force constant and 320 kHz resonant frequency (Nanosensors TM, Neuchâtel, Switzerland). Inspection of the surface profile was carried out on an x-y accessible 1×1 μm area at 0.5 Hz scan rate with XEP and XEI software for data acquisition and image processing.

2.4 Electrochemical Characterization Studies

Electrochemical inspections were done at room temperature on a 50 μl droplet of an electrolyte solution at the working electrode surface area. A solution of 0.05 M PBE containing 1.0 mM $K_3Fe(CN)_6$ at pH 6.5 was used as the basal electrolyte reagent throughout all experiments. Electrochemical impedance spectroscopy (EIS) measurements were performed in potentiostatic state as a single sine wave at a frequency range of $0.01–10^5$ Hz and a frequency number of 50 with the amplitude of 10 mV and estimated duration of 6 minutes. Cyclic voltammetric (CV) profiles were obtained over the potential scan range from − 0.6 to + 0.6 V at a scan rate of 25, 50, 100, 150 and 200 mVs^{-1}. Linear sweep voltammetry (LSV) was carried out at similar potential scan range at a scan rate of 50 mVs^{-1}.

2.5 Enzyme Activity Determination

The GST enzyme activity was determined in accordance of an approved procedure [4] using a substrate solution containing 1 mM reduced GSH and 1 mM CDNB in 0.05 M PBE at pH 6.5 as an electrolyte for electrochemical sensing of the prepared SPCE-Chi-GST biosensor. Standard calibration of captan was acquired by fortifying authentic captan at various concentrations ranged from 0 - 20 μg/ml and reacting with the substrate solution by 1:1 ratio. The enzyme sensing activity was assessed before and after captan accretion with an incubation period of 15 minutes. Inhibition of enzyme activity was calculated from the rest of current peak obtained by the equation, Inhibition (%) = ((*Ipe* – *Ipf*) / *Ipe*) × 100, where *Ipe* and *Ipf* represent the peak height current of GSH-CDNB reaction product on the SPCE-Chi-GST before and after the addition of captan fungicide, respectively.

3. RESULTS AND DISCUSSION

3.1 Morphological Characteristics of the Prepared Electrode Working Surfaces

The surface morphology of each working electrode type could be manifested directly by their topographic inspection under atomic force microscope. Typical AFM images in three dimensions from the nanoscale surface scanning are as shown in Fig. 1 which representing the original SPCE in image A, the chitosan modified electrode (SPCE-Chi) in image B and the SPCE-Chi that was immobilized with GST enzyme (SPCE-Chi-GST) in image C. It appears that the chitosan nanoparticle layer is thoroughly covered onto SPCE basement upon this surface modification (Fig. 1B). On the other hand, a prominent distinction can be realized following the electrode working surface transformation and a conspicuous layer of the GST enzyme bound to the surface after immobilization was apparently formed as shown in image C in Fig. 1. Therefore a successful immobilization of GST enzyme can be stated according to these circumstantiated images.

Fig.1Three-dimensional AFM surface micrographs

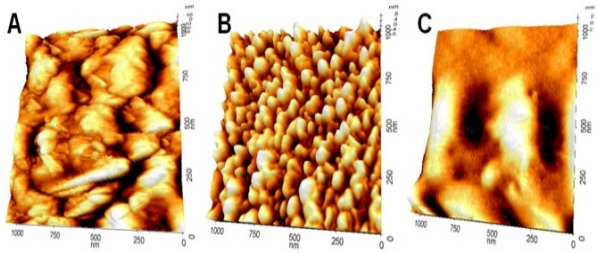

at nanoscale of (A) original bare SPCE, (B) SPCE-Chi, and (C) SPCE-Chi-GST

3.2 Electrochemical Impedance Spectroscopy (EIS)

An EIS assay is exploited to estimate the electrocatalytic properties of original bare SPCE, SPCE-Chi, and SPCE-Chi-GST. Their faradic impedance spectra at a frequency range of 0.01-10^5 Hz are as demonstrated by the nyquist plot that represents a real component impedance (Z') along the x-axis and an imaginary component impedance (Z") along the y-axis with varying frequency from high to low toward the right direction in Fig. 2A with an enlarged view of them at the high-frequency region in Fig. 2B. The spectral character of each could be obviously distinguished and thus signifies the alteration upon stepwise manipulation according to the assumption of Warburg impedance for a semi-infinite diffusion on the smooth surface [6]. In this figure, a broad semicircle at high-frequency range has arisen in the spectra of SPCE as typical characteristic for a high electron transfer resistance. Notable plot from SPCE-Chi is evident by its almost straight line which indicates an extremely fast electron transfer phenomenon due to numerous positive charges holding the quality of the chitosan. While a distinct small semicircle has derived in the spectrum of SPCE-Chi-GST which implied for a deceleration of electron transfer after GST immobilization. The reference impedance model using a modified Randles equivalent circuit in this relationship can be written as *Rs*(*Cdl*(*Rct*(W))) where *Rs* is the cell resistance, *Rct* is the charge transfer resistance, *Cdl* is double-layer capacitance and W is the Warburg element. The impedance-resistance values could be approximated to be 187, 385 and 346 Ωcm^{-2} for *Rs*, and 4,697, 395 and 483 Ωcm^{-2} for *Rct* in bare SPCE, SPCE-Chi and SPCE-Chi-GST, respectively. It seems that the stepwise manipulation of SPCE working surface led to an increase in *Rs* due to a change in the current flow path within the cell system by a covered layer of the differentiated electrode surface. While the *Rct* of SPCE-Chi appears to decrease down to almost 12 folds in corresponding to an expedite activity of the Fe^{3+}/Fe^{2+} redox couple by the influence of chitosan assembly onto the original SPCE surface. A bit raised up in *Rct* value than the basal SPCE-Chi has been observed after an immobilization of GST enzyme to make the SPCE-Chi-GST. This incidence probably informs the presence of a barrier that resulted from negative charges repulsion of the enzyme which retarded the electrolyte $[K_3Fe(CN)_6]^{3-/4-}$ redox action and detained the ion charges associated to a successful GST immobilization on SPCE-Chi surface.

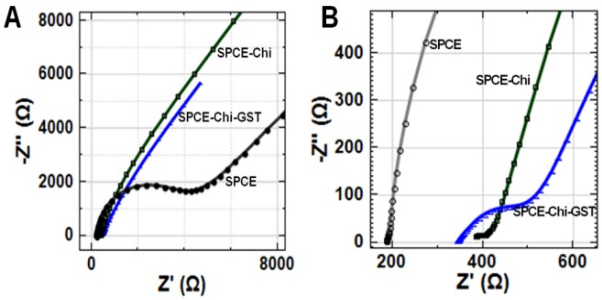

Fig. 2 Impedance spectra of SPCE, SPCE-Chi and SPCE-Chi-GST in 0.1 M PBE (pH 6.5) containing 1.0 mM $[K_3Fe(CN)_6]^{3-/4-}$ at frequency range: 0.1–100,000 Hz, AC potential: 0.01 V, bias potential: 0.18 V revealed by nyquist plots (A) and the enlarge view (B).

3.3 Cyclic Votammetric Characterization

A one-electron transfer reduction of ferricyanide to ferrocyanide model system was employed for an elucidation of the electrode

performance by cyclic voltammetry using 1.0 mM $K_3Fe(CN)_6$ in 0.05 M PBE as a probe [7]. Typical peak curve of the reductive and reverse oxidative current vs. electrode potential indicating ideal reversible reaction governed by freely diffusion of Fe^{+3}/Fe^{+2} to the planar surface was gained in each electrode at about 0.09 to 0.21 V with the peak separation around 0.1 V at 100 mV s^{-1} scan rate and a potential window of −0.6 to 0.6 V as shown in Fig.3. The oxidation/reduction peak currents of SPCE-Chi and SPCE-Chi-GST were almost 2-3 times bigger than that of original bare SPCE (curve a) as a successive superb improvement in electroactive response due to the surface furnishing by an enriched cationic chitosan biopolymer [8, 9, 10]. A high rate of electron transfer process was thus accelerated via this highly conductive chitosan composing as demonstrated by the curve b for SPCE-Chi and curve c for SPCE-Chi-GST. Even though a bit smaller peak current curves were appeared due to a small electron transfer deducted by subsequent GST enzyme immobilization stepwise. The values of electrochemical parameters correlated to this cyclic voltammogram figure were summarized in Table 3. Differentiation in the measured values was remarked among these electrodes such as an increase of the peak potential separation ($\triangle Ep$), the potential of full width at half peak height (E_{fwhm}) and the half-wave potential ($E_{1/2}$). This evidence betokened the formation of extra layer and network on the ground surface following the stepwise manipulation. The calculated ratio between anodic and cathodic peak currents (I_{pa}/I_{pc}) in SPCE and SPCE-Chi were 0.99 and 0.95 and although a bit dropped to 0.84 in SPCE-Chi-GST, all still closed to 1, a value for good diffusion effect. These two peak currents were also directly proportional to the square root of the scan rate ($\upsilon^{1/2}$) with the regression coefficient around 0.99 in every case as a clue for an indication of reversible diffusion control redox process as well. Graphical plots in Fig. 4 illustrate the representative cyclic voltammogram of an electrochemical responding to scan rate effect including their linear regression relationship from SPCE-Chi-GST.

The electroactive area of the electrodes were determined according to the Randles–Sevcik equation [11] for mass transfer in reversible diffusion-controlled systems as $I_p = (2.69 \times 10^5)n^{3/2}ACD^{1/2}v^{1/2}$, where I_p is the anodic (I_{pa}) or cathodic (I_{pc}) current peak (in amperes), n is the number of electrons transfer in the redox reaction, A is the electroactive area of the electrode, C is the concentration of $K_3(FeCN)_6$, D is the diffusion coefficient (6.5×10^{-6} cm^2 s^{-1}), and v is the scan rate (in V s^{-1}). The values concluded in Table 1 indicate a great enhance in effective electron transfer area in SPCE-Chi than the original SPCE one, although it is incidentally lessened by an attachment of GST enzyme in SPCE-Chi-GST. The surface coverage of GST immobilized on SPCE-Chi could then be estimated to be 5.53×10^{-12} mol cm^{-2} from this electroactive area (A) using the basic equation of Langmuir model as: $I_a = (n^2F^2 / 4RT)\Gamma Av$, where F is the Faraday constant in coulomb mol^{-1}, R is the gas constant in joule mol k^{-1}, T is the temperature in Kelvin, and Γ is the surface coverage in mol cm^{-2} [12].

The results from cyclic voltammetry on the confirmation of self-assembled layers were in agreement with those from EIS that inferred an efficient electrochemical catalytic activity after the stepwise preparation. Therefore this prepared SPCE-Chi-GST is capable to use for the further study on captan detection.

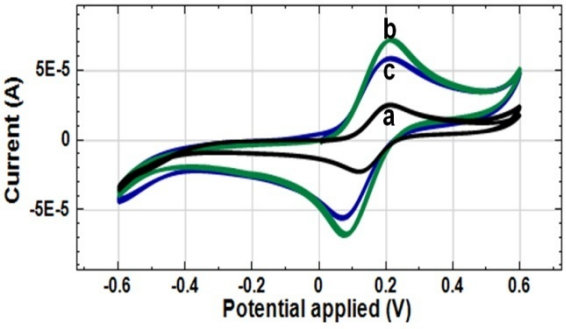

Fig.3 Cyclic voltammograms (CV) of (a) bare SPCE, (b) SPCE-Chi and (c) SPCE-Chi-GST in the basal electrolyte, 0.1 M PBE (pH 6.5) containing 1.0 mM $[K3Fe(CN)6]^{3-/4-}$ as the redox probe at 100 mV s^{-1} scan rate.

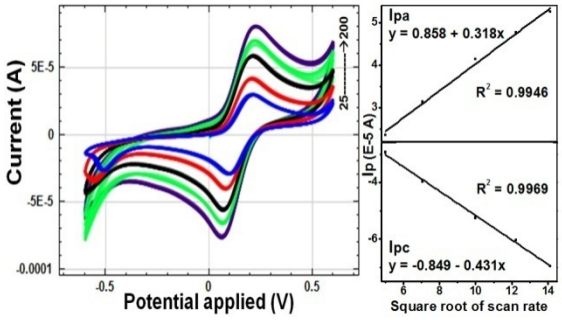

Fig. 4 CV of SPCE-Chi-GST in the basal electrolyte 0.1 M PBE (pH 6.5) containing 1.0 mM [K3Fe(CN)6]3−/4− accounted by curves from inner to outer corresponding to 25, 50, 100, 150 and 200 m·Vs^{-1} scan rates, respectively, with their coordinate linear relationship of anodic and cathodic peak current vs. square root of scan rate on the right plots.

Table 1 Electrochemical parameter values of the prepared electrodes from cyclic voltammogram at 100 mV s^{-1} scan rate shown in Fig. 3

Parameters	SPCE	SPCE-Chi	SPCE-Chi-GST
$\triangle Ep$ (V)	0.086	0.102	0.108
E_{fwhm} anode (V)	0.155	0.184	0.191
E_{fwhm} cathode (V)	0.155	0.180	0.208
$E_{1/2}$ anode (V)	0.059	0.078	0.080
$E_{1/2}$ cathode (V)	0.059	0.075	0.079
I_{pa}/I_{pc}	0.99	0.95	0.84
Electroactive area (cm^2)	0.03	0.09	0.08

Note: SPCE = screen printed carbon electrode, SPCE-Chi = chitosan-modified screen printed carbon electrode, SPCE-Chi-GST = GST immobilized chitosan-modified screen printed carbon electrode, $\triangle Ep$ = peak potential separation, E_{fwhm} = potential of full width at half peak height, $E_{1/2}$ = half-wave potential, I_{pa} = anodic peak current, I_{pc} = cathodic peak current (in amperes), V = volt.

3.4 Electrochemical Sensing Mechanisms of SPCE-Chi-GST

The CV profiles of the GST immobilized working electrode, SPCE-Chi-GST, as well as their corresponding bare SPCE and SPCE-Chi were gained in the absence and presence of 2.5 µg/ml captan in 0.1 M PBE (pH 6.5) containing 1.0 mM $[K_3Fe(CN)_6]^{3-/4-}$ with 1 mM reduced GSH and 1 mM CDNB as analytic substrate buffer with scan rate of 100 mV s^{-1} as shown in Fig. 5. In the sole substrate buffer, almost obvious one oxidation and one reduction charging current peaks appeared at E_{pa} of 0.27 V and E_{pc} of 0.16 V owing to the traditional GSH-CDNB conjugation reaction by GST catalysis [13] that can be summarized as CDNB + GSH $\xrightarrow{GST}$ GS-DNB + HCl . The peak separation between them was about 0.1 V indicating profuse diffusion behaviour of the analytic substrate toward the electrode surfaces (Fig. 5 curve a-c). An explicit CV current response was generated in the presence of captan containing analysis buffer in SPCE-Chi-GST with two oxidation and two reduction peaks as seen in Fig. 5 curve d, suggesting a differentiation due to captan catalytic reaction in the system. The first oxidation peak at E_{pa} of 0.12 V and the second oxidation peak at E_{pa} of 0.27 altogether with the other two prominent reduction peaks at E_{pc} of -0.078 V and 0.145V were emerged.

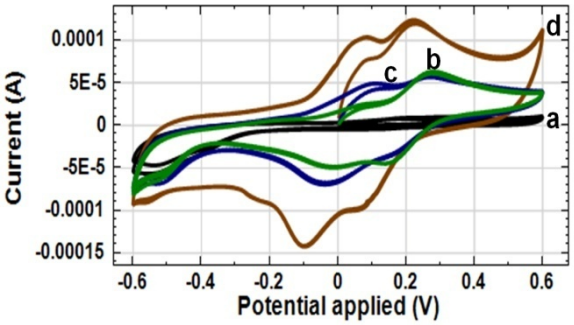

Fig. 5 CV at 100 mV s^{-1} scan rate of (a) bare SPCE, (b) SPCE-Chi-GST, (c) SPCE-Chi-GST in basal electrolyte with 1 mM reduced GSH and 1 mM CDNB analysis buffer as a blank GST enzyme substrate; and of (d) SPCE-Chi-GST in 2.5 µg/ml captan included analysis buffer.

The effect of scan rate on the peak currents and the peak potentials in the presence of captan by the GST immobilized electrodes was illustrated in Fig.6. All the anodic and cathodic peak currents gradually increased with an increase in the scan rate at the observed range of 25–200 mV s^{-1} and a linear relationship between the peak currents and square root of the scan rates with the correlation coefficient R^2 around 0.99 of each was also demonstrated as an evidence for a diffusion controlled process. However, the current peaks for corresponding oxidation and reduction were drifting apart with the increasing scan rate. The I_{pa}/I_{pc} values obtained were about 0.5 for the first oxidation and reduction peak couple and about 1.6 for the second couple. These deflection outcomes were thus accountable for the slow electron transfer manner by the quasi-reversible or irreversible processes circumstance.

According to the postulation of captan reaction mechanism [14, 15], this fungicide reacts extremely rapidly with thiol-containing compounds such as glutathione to produce THPI (1,2,3,6-tetrahydro-phthalimide) and reactive thiophosgene by the equation: Captan + GSH → Thiophosgene + THPI +HCl . The thiophosgene immediately undergoes further reaction with amino and thiol groups of the cysteine moiety contained in the tripeptide glutathione through a xenobiotic-GSH conjugation process by GST catalysis to form a thiazolidine-GSH complex which it is spontaneously transformed to an electroactive thiazolidine ring compound, thiazolidine-2-thione-4-carboxylic acid (TTCA). The last oxidation step is proposed by the equation: Thiophosgene + GSH $\xrightarrow{GST}$ TTCA+2HCl. Considering the GSH oxidation catalysed by GST, the two separated oxidation peaks emergence

following the CV measurement in the presence of captan altogether with universal substrate CDNB thus could be presumed as the occurrence of two different xenobiotic-GSH conjugation complexes from the reaction of GSH with thiophosgene intermediate of captan at the E_{pa} of 0.12 V and from the reaction of GSH with CDNB at the E_{pa} of 0.27 V.

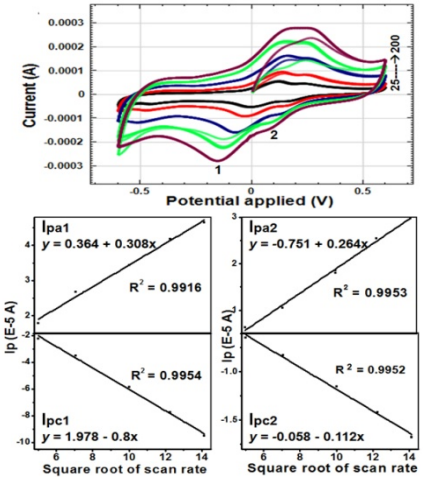

Fig. 6 Cyclic voltammograms of SPCE-Chi-GST in analysis buffer containing 2.5 µg/ml captan accounted by curves from inner to outer corresponding to 25, 50, 100, 150 and 200 m·Vs^{-1} scan rates, respectively, with the coordinate linear relationship of their two anodic (Ipa1 and Ipa2) and two cathodic peak (Ipc1 and Ipc2) currents vs. square root of scan rate.

3.4 Linear Detection Range of Captan

Linear sweep voltammetry (LSV) method was employed to determine the sensing performance of SPCE-Chi-GST at a scan rate of 50 mV s^{-1} in the potential applied range of -0.06 to 0.6 V. The resulting voltammograms were recorded at 0 up to 20 µg/ml captan concentration in basal electrolyte with 1 mM reduced GSH and 1 mM CDNB.

Similar electrochemical behavior to the CV profile was arisen by the appearance of two-step oxidation peaks around the potential position 0.04 to 0.12 V for the first peak that continued growing and around 0.2 to 0.27 V for the second peak that continued decreasing in the presence of varying up captan concentrations as shown in Fig. 7. As the peak 1 (p1) gradually increased with an increase of captan concentration, this behavior could be assumed as a result of the reaction of GSH with thiophosgene intermediate of captan. While the response in the peak 2 (p2) were gradually decreased by typical reaction of GST inhibition.

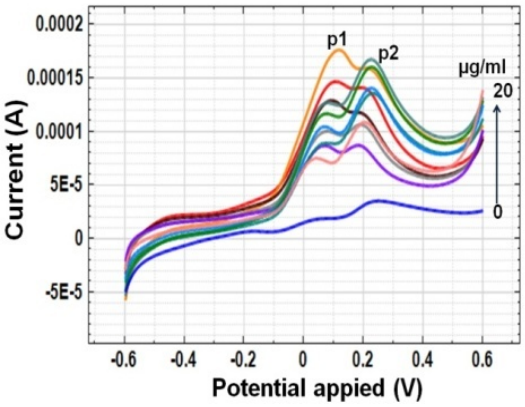

Fig. 7 LSV performance of SPCE-Chi-GST with simultaneous peak 1 (p1) and peak 2 (p2) currents corresponding to different captan concentrations.

Calibration plot and detection limit were thus comparatively calculated from either p1 or p2 current against captan concentration. Fig. 8 demonstrates a linear relationship between the current response of SPCE-Chi-GST and captan concentration in two dynamic ranges of 0 - 1.25 µg/ml and 2.5 - 15 µg/ml in both cases. The growing p1 currents gradually increased with an increase in captan concentration and the obtained linear regression equations can be expressed as $y = (1.613 \pm 0.028) + (0.99 \pm 0.043)x$ with R^2 = 0.974 for the first range, and $y = (2.93 \pm 0.026) + (0.071 \pm 0.003)x$ with R^2 = 0.984 for the second range, where y represents the peak current in e-5 ampere (A) and x represents the captan concentration in µg/ml as seen in Fig 8A segment p1a and p1b. The detection limit (LOD) for captan in this case is estimated to be 0.225 µg/ml based on the formula: LOD = 3S/b where S is the standard deviation (n=15) and b is the slope of the regression. In case of the decreasing p2 currents of typical GST inhibition reaction, their two linear regression equations are $y = (5.066 \pm 0.0199) + (-1.205 \pm 0.027)x$ with R^2 = 0.995 in the captan concentration ranges 0 - 1.25 µg/ml and $y = (2.492 \pm 0.044) + (-0.102 \pm 0.005)x$ with R^2 = 0.977 in the ranges 2.5 - 15 µg/ml. The LOD of 0.198 µg/ml can be acquired in this p2 current case. Notable differences between the slopes of the calibration plots from the first range at 0-1.25 and the second range at 2.5 – 15 µg/ml of captan concentrations in both p1 and p2 currents are probably due to kinetic limitation at the confine electrode surfaces. The slope obtained from the first concentration range is apparently higher because the active sites number containing on the working surface still be excess in relation to the total number of lower analyte molecules. These active sites may gradually become lessen with the increasing number of the analyte molecules at higher concentration and the relative slope hence is decreased. Statistical analysis between the p1 and

p2 current measurements has yielded the value of t_{exp} at 0.69 and F_{exp} at 1.03 in comparison to the null hypothesis student *t*-test of 1.96 critical value and *F*-test of 1.00 critical value (n = 16) at 95% confidence level. As the t_{exp} value was lower than the student *t*-test critical value hence their population means are not significantly different. This result also showed an accuracy of the system. While the F_{exp} gained was around the $F_{critical}$ that should be considered acceptable for the null hypothesis in the population variance. Therefore both the p1 and p2 current delivery cases could be similarly accepted for captan detection.

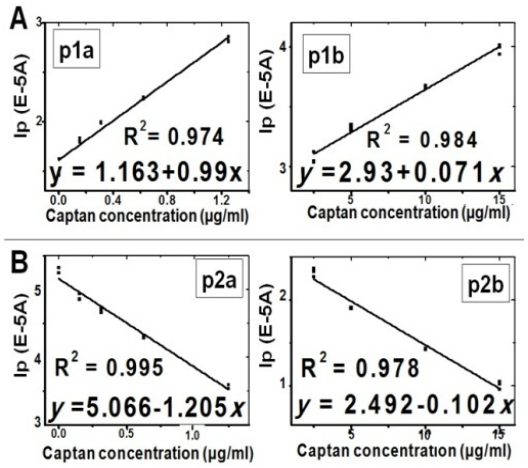

Fig. 8 Linear regression relationships from LSV performance of SPCE-Chi-GST between peak 1 current (A) vs. captan concentration ranged from 0-1.25µg/ml (p1a), and from 2.5-15µg/ml (p1b); and between peak 2 current (B) vs. the range from 0-1.25µg/ml (p2a), and from 2.5-15µg/ml (p2b).

The detection range in every regression performance is comparably more competent than the previous reports based on GST activity that was carried through 0.25 to 16 ppm using aminopropyltriethoxysilane-modified gold electrode [16] and 0 to 2 ppm using optical biosensor system [17]. These repetitive measurement series with different concentrations of captan in all cases gave a correlation coefficient over 0.9 and a relative standard deviation within 3% (n =30), thus demonstrating a high reliability and good repeatability of the measurements including a reproducibility of the SPCE-Chi-GST fabrication.

4. CONCLUSION

In this present study, a facile electrochemical biosensor has been developed for specific and practical determination of captan fungicide. This biosensor is based on the modification of SPCE with biopolymer chitosan and the covalent immobilization with GST enzyme specific to captan catalyzing process. Two sensing mechanisms in this captan determination has been proposed with reference to an occurrence of two simultaneous oxidation peak occurrences in CV and LSV analyses by the formation of two different xenobiotic-GSH conjugation complexes in the reaction system. Quantitative measurements were carried out by their converse concomitance, the peak 1 growing current and the peak 2 decreasing current. A good progressive linear relationship between peak current and captan concentration could be seen in both peak current cases with the LOD around 0.2 µg/ml. All calibrations were attested to be high reliability and reproducibility with the RSD lower than 3% and the correlation coefficient above 0.9. Therefore the detection and quantification of captan are enabled by newly proposed peak 1 current as well as the traditional peak2 current and suitable confirmation of the gaining results could be achieved in parallel. Correlatively, the gratify performances of SPCE-Chi-GST have allowed the promising development of a specific biosensor for convenient practice and fast routine sensing in real instances.

5. ACKNOWLEDGEMENTS

The authors gratefully acknowledge Khon Kaen University's Division of Research and Technology Transfer Affair for partial funding to both individual and research group (KKU-56-57) in Biosensing Technology and the KKU Research Instrument Center for all facilities. We also thank Miss Kwandao Sigalang and Miss Karinthorn Srichankam for their assistance in the lab.

6. REFERENCES

[1] Edwards R, Ferry DG, Temple WA. (1991). "Fungicides and related compounds", Handbook of Pesticide Toxicology, Vol. 3, Hayes WJ Jr, Laws ER Jr, Eds.New York: Academic Press, 1991, pp. 1409–1470.

[2] Gottzein AK, Musshoff F, Madea B, "Systematic toxicological analysis revealing a rare case of captan ingestion", J. of Forensic Sciences, Vol. 58, Jul. 2013, pp. 1099-1103.

[3] Stevens JT, Breckenridge C,"Crop protection chemical", Principle and Methods of Toxicology, Hayes A, Ed. Philadelphia: Taylor &Francis, 2001, pp. 565- 684.

[4] Gordon EB, "Captan and folpet", Handbook of Pesticide Toxicology, Krieger RI, Ed. New York: Elsevier, 2010, pp. 1915–1949.

[5] Wongkaew P, Poosittisak S, "Atomic force microscopic and electrochemical characterization of the modified screen-printed carbon electrode by self-assembled

deposition of chitosan and activated carbon", Int. J. of GEOMATE, 11, Aug. 2016, pp. 2356-2362.

[6] Orazem ME, Tribollet B, Electrochemical Impedance Spectroscopy. New York: Wiley, 2008, pp. 1-459.

[7] Nicholson RS, "Theory and Application of Cyclic Voltammetry for Measurement of Electrode Reaction Kinetics", Analytical Chemistry, Vol. 37, Apr.1965, pp.1351-1355.

[8] Wongkaew P, Poosittisak S, "Electro-affinity of SCWL-dsDNA on different high deacetylation degree chitosans deposited glassy carbon electrode", Advances in Developing Affordable In-Vitro Molecular Diagnostics, Puri CP, Abidi N, Bhanushali, P, Pere A, Gupta SK, Eds. Mumbai: Yashraj Research Foundation, 2012, pp. 249-258.

[9] Wongkaew P, Poosittisak S, "Diagnosis of sugarcane white leaf disease using the highly sensitive DNA based voltammetric electrochemical determination" Amer. J. of Plant Sci., Vol.5, Jul. 2014, pp. 2256-2268.

[10] Liu Y, Gaskell KJ, Chen Z, Yu LL, Pay GF, "Chitosan-coated electrodes for bimodal sensing: selective post-electrode film reaction for spectroelectrochemical analysis", Langmuir, Vol. 24, Jun. 2008, pp. 7223-7231.

[11] Bard AJ, Faulkner LR, "Electrochemical Methods: Fundamentals and Applications", 2nd ed., New York: Wiley, 2000, pp. 1-864.

[12] Prodomidis MI, Florou AB, Tzouwara-Karayanni SM, Karayannis MI, "The importance of surface coverage in the electrochemical study of chemically modified electrodes", Electroanalysis, Vol. 12, Dec. 2000, pp. 1498-1501.

[13] Van der Aar EM, de Groot MJ, Bouwman T, Bijloo GJ, Commandeur JN, Vermeulen NP. "4-Substituted 1-chloro-2-nitrobenzenes: structure-activity relationships and extension of the substrate model of rat glutathione S-transferase 4-4", Chem. Res. of Toxicology, Vol. 10, Apr. 1997, pp. 439-449.

[14] Wolfe NL, Zepp RG, Doster JC, Hollis RC,"Captan hydrolysis", J. of Agricultural and Food Chemistry, Vol. 24, May 1976, pp. 1041–1045.

[15] Berthet A, Bouchard M, Danuser B, "Toxicokinetics of captan and folpet biomarkers in orally exposed volunteers", J. of Applied Toxicology, Vol. 32, Mar. 2012, pp. 194-201.

[16] Singh RP, Kim YJ, Oh BK, Choi JW, "Glutathione-s-transferase based electrochemical biosensor for the detection of captan", Electrochemistry Communications, Vol. 11, Jan. 2009, pp.181–185.

[17] Choi JW, Kim YK, Oh BK, Song SY, Lee WH, "Optical biosensor for simultaneous detection of captan and organophosphorus compounds", Biosensors and Bioelectronics, Vol. 18, May 2003, pp. 591-597.